Nanoparticles

DOI: 10.1002/anie.201202085

Microwave-Assisted Synthesis of Biofunctional and Fluorescent Silicon Nanoparticles Using Proteins as Hydrophilic Ligands**

Yiling Zhong, Fei Peng, Xinpan Wei, Yanfeng Zhou, Jie Wang, Xiangxu Jiang, Yuanyuan Su, Shao Su, Shuit-Tong Lee, and Yao He**

Silicon nanomaterials are important nanomaterials and have been extensively studied and explored for myriad applications ranging from electronics to biology.[1] Fluorescent silicon nanoparticles (SiNPs) are potentially ideal fluorescent probes for biological and biomedical studies owing to their favorable biocompatibility and low toxicity. However, most SiNPs are not well water-dispersible since their surfaces are covered by hydrophobic moieties (e.g., styrene, alkyl, and octene).[2] To realize aqueous dispersibility of SiNPs, extensive efforts have been devoted to modify SiNP surfaces with hydrophilic species.[3,4] While the exciting progresses offer versatile strategies for fabrication of water-dispersible SiNPs, much work is still required to enable wide-ranging bioapplications. In particular, the current methods often invoke relatively complicated manipulations. At least two independent procedures are generally required, that is, in the first step hydrophobic SiNPs are prepared and subsequently these are modified with hydrophilic moieties (e.g., acrylic acid, allylamine, polymer, phospholipid micelles, etc.).[3,4] Moreover, for any immunoassay-related applications (e.g., immunofluorescent bioimaging, tumor-specific targeting), the SiNPs must be conjugated with proteins.[3–6] As is well-known, bioconjugation procedures (e.g., the cross-linking reaction using *N*-(3-dimethylaminopropyl)-*N*′-ethylcarbodiimide hydrochloride (EDC) and *N*-hydroxysuccininmide (NHS)) are complicated, time-consuming (several hours are needed at least), and require additional processing steps. Furthermore, optical properties and stability of the modified SiNPs are prone to deteriorate during treatment.[3,4,6]

Herein, we present a facile microwave-assisted strategy for preparation of biofunctional and fluorescent SiNPs by using proteins as hydrophilic ligands. Briefly, silicon nanowires (SiNWs), which were prepared by using an established HF-assisted etching method, first break up into SiNPs in a specialized microwave reactor at high reaction temperature (180–200 °C). Afterwards, the resultant SiNPs are further modified with immunoglobulin G (IgG, a typical protein) under mild microwave heating after addition of the protein as hydrophilic ligand. Note that, to avoid protein degradation, we employed short-time (ca. 5–10 min) and low-temperature (30 °C) microwave irradiation in our experiment. As a result, IgG-modified SiNPs can be rapidly prepared using a short reaction time (e.g., 15 min; see experimental details in the Supporting Information). The as-prepared SiNPs show strong fluorescence (photoluminescent quantum yield (PLQY): 18 %), robust photostability, pH-stability, and storage stability, and favorable biocompatibility. Remarkably, the SiNPs feature excellent aqueous dispersibility and biospecific properties owing to a large number of protein molecules on the surface. Our experiment further demonstrates that such SiNPs could be directly employed for immunofluorescent cellular targeting, without requiring additional bioconjugation.

Figure 1 a presents the transmission electron microscopy (TEM) image of the as-prepared SiNPs, appearing as spherical particles with good monodispersity. Moreover, the well-resolved lattice planes of approximately 0.15 nm spacing in the high-resolution TEM (HRTEM) image (inset in Figure 1 b) demonstrates the excellent crystalline structure of the prepared SiNPs. The size distribution in Figure 2 a, calculated by measuring more than 250 particles in the TEM image, shows the SiNPs have an average size of (3.17 ± 0.53) nm in the TEM image (see enlarged TEM and HRTEM images in Figures S1 and S2 in the Supporting Information). Note that water in the SiNP sample must be strictly removed for TEM characterization, and protein

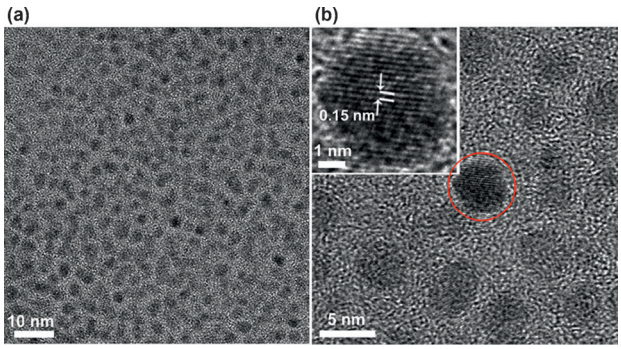

Figure 1. a) TEM and b) HRTEM images of the as-prepared SiNPs. Inset in (b) presents the enlarged HRTEM image of a single SiNP.

[*] Dr. Y. L. Zhong, F. Peng, X. P. Wei, Y. F. Zhou, J. Wang, X. X. Jiang, Dr. Y. Y. Su, S. Su, Prof. S. T. Lee, Prof. Y. He
Institute of Functional Nano & Soft Materials (FUNSOM) and Jiangsu Key Laboratory for Carbon-based Functional Materials & Devices, Soochow University
Suzhou 215123 (China)
E-mail: apannale@cityu.edu.hk
yaohe@suda.edu.cn

[**] This work was supported by the National Basic Research Program of China (973 Program 2012CB932400), NSFC (30900338, 51072126), and the Research Grants Council of HKSAR (CityU5/CRF/08, N_CityU108/08, and CityU 101608). We thank Dr. Feng Bao for his technical assistance.

Supporting information (including experimental details, Figures S1–S8, and corresponding discussion) for this article is available on the WWW under http://dx.doi.org/10.1002/anie.201202085.

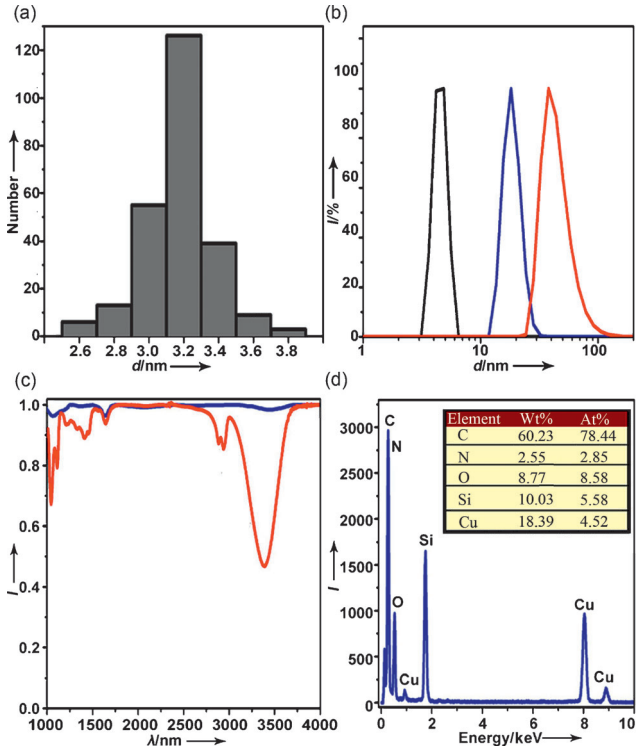

Figure 2. a) The size distribution of the prepared SiNPs. b) Dynamic light scattering (DLS) histogram of pure SiNPs without IgG proteins as ligands (black trace), pure IgG (blue trace), and the prepared SiNPs with IgG as ligands (red trace). c) FTIR spectra of the free SiNWs (blue trace) and the prepared SiNPs (red trace). d) Energy-dispersive X-ray spectroscopy (EDX) pattern of the SiNP samples. Table in inset presents the elemental ratios (weight and atom percentages) calculated by the EDX software (K-shell intensity ratios are indicated).

ligands are thus hardly observed by TEM owing to low contrast. In contrast, the SiNP sample in the aqueous phase can be directly measured, and protein molecules are readily detected by dynamic light scattering (DLS), making it feasible to determine actual sizes of the prepared SiNPs in aqueous solution.[7] Therefore, we performed DLS characterization. Notably, the size of the prepared SiNPs determined by DLS (ca. 40 nm) is distinctly larger than the corresponding size measured by TEM (red line in Figure 2b). As a control, the size determined by DLS of the pure SiNPs, that is, SiNPs without IgG ligands, is measured to be approximately 5 nm (black line in Figure 2b), which is close to the size observed by TEM of 3.2 nm but is much smaller than that of the prepared SiNPs with IgG ligands, thus indicating that IgG molecules are successfully linked with the prepared SiNPs. Moreover, based on the size measured by DLS (ca. 18 nm) of IgG molecules (blue line in Figure 2b), we thus estimate around four IgG molecules are attached to one SiNP.

To show the changes of the dominant chemical bonding that has occurred during the reaction, the FTIR spectra of the pure SiNWs (Figure 2, blue line) and prepared SiNPs (red line) were measured. Significantly, in contrast to the feeble absorption of SiNWs, the SiNPs feature several distinct absorption peaks ranging from 1000 to 4000 cm^{-1}. Typically, sharp absorbance peaks at approximately 1000–1150 cm^{-1} are ascribed to the vibration stretch of Si–O bonding, thereby indicating that many Si–O bonds are formed under microwave irradiation.[4d,e,8] Moreover, absorbances of 1210–1320, 1390–1440, 1600–1680, and 2800–3000 cm^{-1}, which are assigned to the O–H bond (deformation vibration), C–O bond (bending vibration), C=O bonds (stretching vibration), and O–H bond (stretching vibration), respectively, indicate abundant carboxylic acid groups in the prepared SiNPs.[4e,9] Notably, a distinct absorption peak at approximately 3290 cm^{-1}, which is attributed to the stretching vibration of an N–H bond, provides convincing evidence that the resultant SiNPs have a large number of amino groups.[10] The EDX pattern provides the elemental ratio, revealing that the SiNPs contain Si, O, and N with 10.03%, 8.77%, and 2.55% weight concentration, respectively (Figure 2d). Note that the C and Cu weight concentrations listed in the table are not reliable since carbon-coated copper grids are used for the EDX test.

Figure 3a shows the resultant SiNPs possess good optical properties with a resolved absorption peak and a strong luminescence peak (maximum emission wavelength at ca. 660 nm). Moreover, the aqueous sample of the SiNPs displays distinct red luminescence under UV irradiation, thereby further demonstrating the strong fluorescence of the as-prepared SiNPs (Figure 3b). Significantly, whereas the precursor solution with dispersed SiNWs is severely turbid, the aqueous solution of SiNPs is transparent in ambient light (Figure 3c). This experiment clearly shows that the as-prepared SiNPs are highly water-dispersible, owing to the high number of hydrophilic IgG molecules on the surface. Moreover, the SiNPs possess robust pH stability, preserving stable fluorescence at pH values between 4 and 12 (Figure 3d). We attribute the high pH stability to IgG molecules, which contain amino and carboxylic acid groups and take over the role of a buffer. Furthermore, IgG molecules are tightly attached to SiNPs, thereby acting as "protective shell", which improves stability to changes of the pH value.[3c,d,4e] Furthermore, the prepared SiNPs show superior photostability compared to the FITC dye (a conventional fluorescence label), CdTe QDs, and CdSe/ZnS core-shell QDs (recognized as photostable fluorescent labels[5]). The fluorescence of FITC is quickly quenched after three minutes of UV irradiation owing to severe photobleaching (Figure 3e). CdTe QDs preserve approximately 50% of the original PL intensity after ten minutes of UV irradiation, yet their fluorescence is severely quenched after irradiation for additional 15 min. CdSe/ZnS core-shell QDs exhibit better photostability than CdTe QDs owing to protection of the ZnS shell.[4] The CdSe/ZnS QDs retain approximately 50% of the original PL intensity after 40 min UV irradiation. Nevertheless, the fluorescence of ZnS/CdSe QDs becomes undetectable after approximately 80 min owing to surface deterioration under intense UV irradiation.[11] In sharp contrast, the fluorescence intensity of SiNPs decreases only slightly, and approximately 80% of the initial intensity are retained after 120 min of UV irradiation. We attribute such remarkable photostability to the protection from the ligand shell and the unique PL properties of SiNPs;[12] the photostability is similar to those of the reported acrylic acid/allylamine-capped and polymer-coated SiNPs.[3a,b,4d,e] Furthermore, the prepared SiNPs pos-

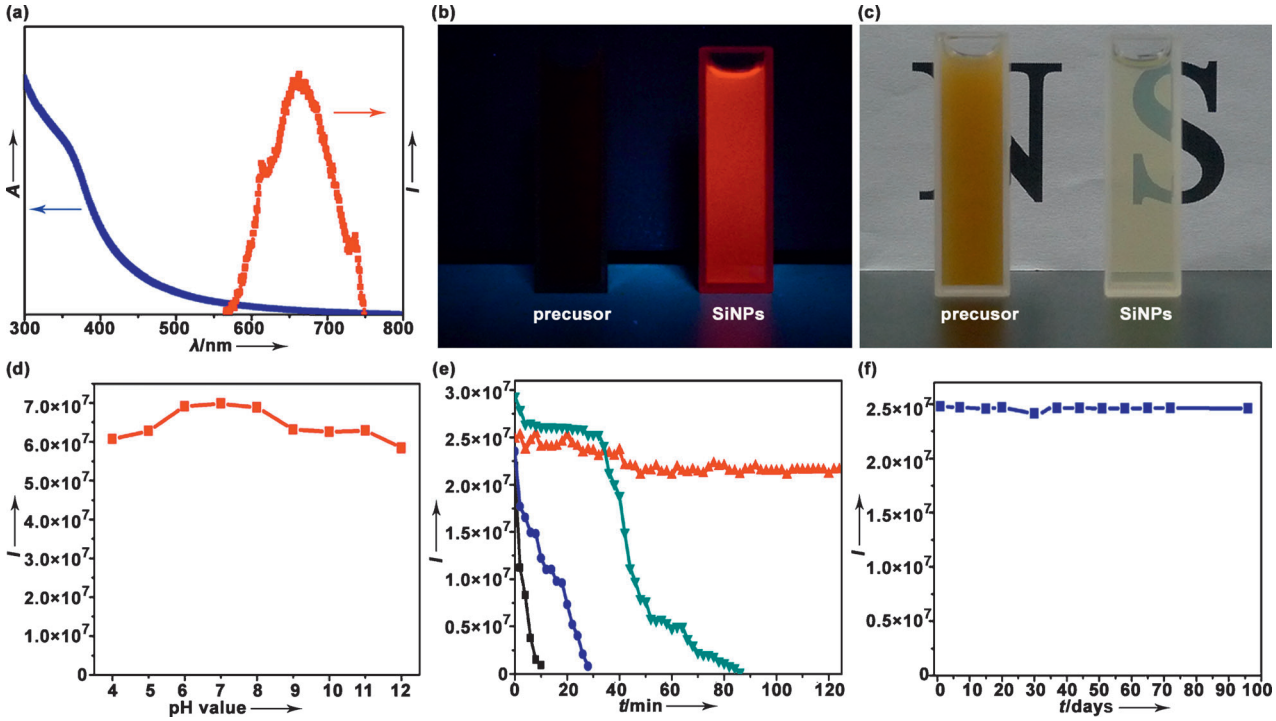

Figure 3. a) Absorption (blue) and photoluminescence (UV-PL, red) spectra of the as-prepared SiNPs. b, c) Photographs of reaction precursor (left), that is, aqueous dispersion of free SiNWs and IgG, and aqueous sample of as-prepared SiNPs (right) under 365 nm irradiation (b) or ambient light (c). d) Temporal evolution of fluorescence of the SiNPs at various pH values. e) Comparison of the photostability of fluorescein isothiocyanate (FITC; black ■), CdTe quantum dots (CdTe QDs; blue ●), CdSe/ZnS QDs (cyan ▼), and as-prepared SiNPs (red ▲). All samples are continuously irradiated by a 450 W xenon lamp. f) Temporal evolution of fluorescence of the SiNPs during storage for three months.

sess robust storage stability and maintain strong and stable fluorescence for more than three months when stored in ambient environment (Figure 3 f). To assess the possible use of SiNPs in complex biological environment, we further tested their fluorescence stability in biological medium. Notably, the SiNPs preserve stable fluorescence in Dulbecco's modified Eagle's medium (DMEM) containing 10% fetal bovine serum (FBS) at 37°C (Figure S4 in the Supporting Information); this medium is one of the most commonly used cell culture media. In addition to high pH stability, photostability and storage stability, the as-prepared SiNPs exhibit little cytotoxicity owing to favorable biocompatibility of bulk silicon (Figure S5 in the Supporting Information).[3,4]

The prepared SiNPs are further explored as high-performance bioprobes for immunofluorescence cellular imaging. Hela cells, typical cervical cancer cells, are selected as a model in our studies. Notably, to prove that the resultant SiNPs could be directly used for immunofluorescence targeting, the cells are preincubated with a microtubules-specific anti-tubulin antibody. Indeed, the microtubules of Hela cells are specifically labeled by the prepared SiNPs, since IgG molecules on the SiNPs are highly specific for the anti-tubulin antibody owing to antibody–antigen immunoreactions.[11,4e] As a result, the microtubules targeted by the SiNPs show intense and clearly spectrally resolved red signals (Figure 4 a). As a control, Hela cells are incubated with pure SiNPs, i.e., SiNPs without IgG as ligands, under the same experimental conditions. In striking contrast, the pure SiNPs are non-specifically absorbed by the cells in the absence of IgG; relatively uniform red fluorescence signals can be seen in the whole cellular region (Figure 4 b). This experiment demonstrates that the as-prepared SiNPs are capable of immunofluorescence biological labeling without additional protein conjugation (see enlarged images of immunofluorescent cellular labeling in Figure S6 in the Supporting Information). Moreover, the resultant SiNPs are superbly suitable for long-term cellular imaging. The red signals of the SiNPs are extremely stable during 180 min continuous observation under laser-scanning confocal microscopy (Figure 5 a), since the fluorescent SiNPs feature excellent photostability, in well agreement with previous reports.[3a,b,4] In striking contrast, the signals of the control groups using the CdTe QDs or FITC as fluorescent labels almost completely disappear after irradiation for short time periods (Figure 5 b, c). Specifically, the green fluorescence of FITC rapidly diminishes in three minutes owing to severe photobleaching (Figure 5 c), while the red signals of CdTe QDs are obviously depressed and become feeble after irradiation for 25 min (Figure 5 b), although they display bright and spatially resolved luminescence in the initial ten minutes, because of their greater photostability compared to FITC.

To summarize, we developed a facile one-pot method, which can rapidly prepare high-quality SiNPs by using proteins as hydrophilic ligands. Significantly, the as-prepared SiNPs are strongly luminescent, highly stable, and biocompatible. Moreover, the SiNPs feature excellent aqueous

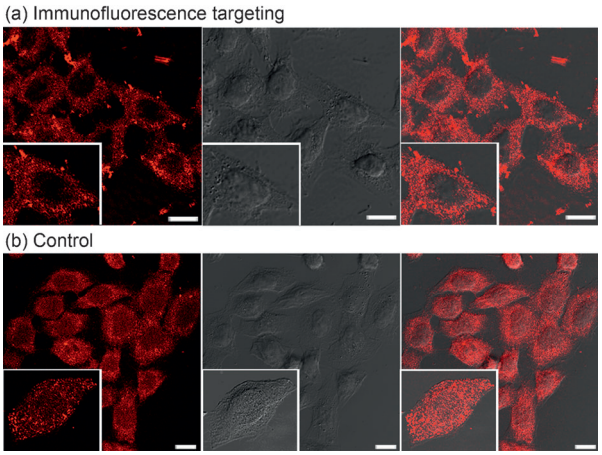

Figure 4. Cell images obtained by using laser-scanning confocal microscopy. a) Microtubules are specifically targeted by the prepared SiNPs, showing strong red fluorescence signals. b) As a control, pure SiNPs, i.e. SiNPs without IgG proteins as ligands, are nonspecifically absorbed by Hela cells. The red signals are distributed in the whole cellular region. Scale bar = 10 μm. Insets present one single cell imaged using the prepared SiNPs (a) and pure SiNPs (b). Left panel shows 488 nm excitation images, middle panel shows bright field images, right panel shows superposition of fluorescence and transillumination images.

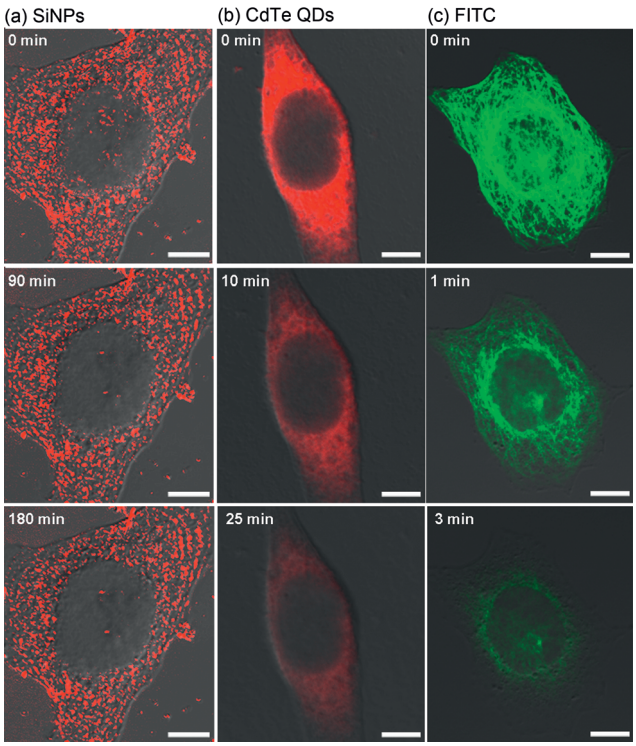

Figure 5. Stability comparison of fluorescence signals of Hela cells specifically labeled with a) SiNPs, b) CdTe QDs, and c) FITC. Scale bar = 5 μm.

dispersibility and biospecific properties owing to their protein-covered surface. The SiNPs can be facilely employed for long-term immunofluorescence labeling without requiring additional complicated protein conjugation. Consequently, the present SiNPs may serve as high-performance biological probes for various biosensing and bioimaging applications. Moreover, by using the described synthesis method, silicon nanomaterials can be readily modified with various proteins with desirable biological properties, since most proteins contain both carboxylic acid and amino functional groups. The present synthetic strategy offers exciting new avenues for designing multifunctional SiNPs and related silicon nanostructures (e.g., nanowire, nanorod, etc).

Received: March 16, 2012
Revised: June 6, 2012
Published online: July 4, 2012

Keywords: fluorescence · imaging agents · nanoparticles · proteins · silicon

[1] a) L. Pavesi, L. D. Negro, C. Mazzoleni, G. Franzo, F. Priolo, *Nature* **2000**, *408*, 440–444; b) Z. F. Ding, B. M. Quinn, S. K. Haram, L. E. Pell, B. A. Korgel, A. J. Bard, *Science* **2002**, *296*, 1293–1297; c) D. D. D. Ma, C. S. Lee, F. C. K. Au, S. Y. Tong, S. T. Lee, *Science* **2003**, *299*, 1874–1877; d) J. E. Allen, E. R. Hemesath, D. E. Perea, J. L. Lensch-Falk, Z. Y. Li, F. Yin, M. H. Gass, P. Wang, A. L. Bleloch, R. E. Palmer, L. J. Lauhon, *Nat. Nanotechnol.* **2008**, *3*, 168–173; e) Y. He, S. Su, T. T. Xu, Y. L. Zhong, J. A. Zapien, J. Li, C. H. Fan, S. T. Lee, *Nano Today* **2011**, *6*, 122–130; f) S. Su, X. P. Wei, Y. L. Zhong, Y. Y. Guo, Y. Y. Su, Q. Huang, S. T. Lee, C. H. Fan, Y. He, *ACS Nano* **2012**, *6*, 2582–2590; g) Y. Y. Su, X. P. Wei, F. Peng, Y. L. Zhong, Y. M. Lu, S. Su, T. T. Xu, S. T. Lee, Y. He, *Nano Lett.* **2012**, *12*, 1845–1850.

[2] a) A. G. Cullis, L. T. Canham, *Nature* **1991**, *353*, 335–338; b) W. L. Wilson, P. F. Szajowski, L. E. Brus, *Science* **1993**, *262*, 1242–1244; c) C. S. Yang, R. A. Bley, S. M. Kauzlarich, H. W. H. Lee, G. R. Delgado, *J. Am. Chem. Soc.* **1999**, *121*, 5191–5195; d) N. M. Park, C. J. Choi, T. Y. Seong, S. J. Park, *Phys. Rev. Lett.* **2001**, *86*, 1355–1357; e) L. Mangolini, E. Thimsen, U. Kortshagen, *Nano Lett.* **2005**, *5*, 655–659.

[3] a) Z. F. Li, E. Ruckenstein, *Nano Lett.* **2004**, *4*, 1463–1467; b) J. H. Warner, A. S. Hoshino, K. J. Yamamoto, R. D. Tilley, *Angew. Chem.* **2005**, *117*, 4626–4630; *Angew. Chem. Int. Ed.* **2005**, *44*, 4550–4554; c) F. Erogbogbo, K. T. Yong, I. Roy, G. X. Xu, P. N. Prasad, M. T. Swihart, *ACS Nano* **2008**, *2*, 873–878; d) F. Erogbogbo, K. T. Yong, I. Roy, R. Hu, W. C. Law, W. W. Zhao, H. Ding, F. Wu, R. Kumar, M. T. Swihart, P. N. Prasad, *ACS Nano* **2011**, *5*, 413–423; e) A. Shiohara, S. Hanada, S. Prabakar, K. Fujioka, T. H. Lim, K. J. Yamamoto, P. T. Northcote, R. D. Tilley, *J. Am. Chem. Soc.* **2010**, *132*, 248–253; f) T. M. Atkins, A. Thibert, D. S. Larsen, S. Dey, N. D. Browning, S. M. Kauzlarich, *J. Am. Chem. Soc.* **2011**, *133*, 20664–20667; g) K. Sato, S. Yokosuka, Y. Takigami, K. Hirakuri, K. Fujioka, Y. Manome, H. Sukegawa, H. Iwai, N. Fukata, *J. Am. Chem. Soc.* **2011**, *133*, 18626–18633; h) M. L. Mastronardi, F. Maier-Flaig, D. Faulkner, E. J. Henderson, C. Kübel, U. Lemmer, G. A. Ozin, *Nano Lett.* **2012**, *12*, 337–342; i) M. Guan, W. D. Wang, E. J. Henderson, Ö. Dag, C. Kübel, V. S. K. Chakravadhanula, J. Rinck, I. L. Moudrakovski, J. Thomson, J. McDowell, A. K. Powell, H. X. Zhang, G. A. Ozin, *J. Am. Chem. Soc.* **2012**, *134*, 8439–8446.

[4] a) Y. He, Z. H. Kang, Q. S. Li, C. H. A. Tsang, C. H. Fan, S. T. Lee, *Angew. Chem.* **2009**, *121*, 134–138; *Angew. Chem. Int. Ed.* **2009**, *48*, 128–132; b) Y. He, Y. Y. Su, X. B. Yang, Z. H. Kang, T. T. Xu, R. Q. Zhang, C. H. Fan, S. T. Lee, *J. Am. Chem. Soc.* **2009**, *131*, 4434–4438; c) Y. He, C. H. Fan, S. T. Lee, *Nano Today* **2010**, *5*, 282–295; d) Y. He, Y. L. Zhong, F. Peng, X. P. Wei, Y. Y.

Su, Y. M. Lu, S. Su, W. Gu, L. S. Liao, S. T. Lee, *J. Am. Chem. Soc.* **2011**, *133*, 14192 – 14195; e) Y. He, Y. L. Zhong, F. Peng, X. P. Wei, Y. Y. Su, S. Su, W. Gu, L. S. Liao, S. T. Lee, *Angew. Chem.* **2011**, *123*, 3136 – 3139; *Angew. Chem. Int. Ed.* **2011**, *50*, 3080 – 3083.

[5] a) D. R. Larson, W. R. Zipfel, R. M. Williams, S. W. Clark, M. P. Bruchez, F. W. Wise, W. W. Webb, *Science* **2003**, *300*, 1434 – 1436; b) X. Y. Wu, H. J. Liu, J. Q. Liu, K. N. Haley, J. A. Treadway, J. P. Larson, N. F. Ge, F. Peale, M. P. Bruchez, *Nat. Biotechnol.* **2003**, *21*, 41 – 46; c) J. K. Jaiswal, H. Mattoussi, J. M. Mauro, S. M. Simon, *Nat. Biotechnol.* **2003**, *21*, 47 – 51; d) X. H. Gao, Y. Y. Cui, R. M. Levenson, L. W. K. Chung, S. M. Nie, *Nat. Biotechnol.* **2004**, *22*, 969 – 976; e) I. L. Medintz, H. T. Uyeda, E. R. Goldman, H. Mattoussi, *Nat. Mater.* **2005**, *4*, 435 – 446.

[6] a) S. P. Wang, N. Mamedova, N. A. Kotov, W. Chen, J. Studer, *Nano Lett.* **2002**, *2*, 817 – 822; b) Y. Xing, Q. Chaudry, C. Shen, K. Y. Kong, H. E. Zhau, L. W. Chung, J. A. Petros, R. M. O'Regan, M. V. Yezhelyev, J. W. Simons, M. D. Wang, S. M. Nie, *Nat. Protoc.* **2007**, *2*, 1152 – 1165.

[7] a) H. C. Fischer, L. C. Liu, K. S. Pang, W. C. W. Chan, *Adv. Funct. Mater.* **2006**, *16*, 1299 – 1305; b) S. S. Banerjee, D. H. Chen, *Chem. Mater.* **2007**, *19*, 6345 – 6349; c) T. S. Hauck, R. E. Anderson, H. C. Fischer, S. Newbigging, W. C. W. Chan, *Small* **2010**, *6*, 138 – 144.

[8] a) J. L. He, Y. Ba, C. I. Ratcliffe, J. A. Ripmeester, D. D. Klug, J. S. Tse, K. F. Preston, *J. Am. Chem. Soc.* **1998**, *120*, 10697 – 10705; b) Y. Kato, H. Yamazaki, M. Tomozawa, *J. Am. Ceram. Soc.* **2001**, *84*, 2111 – 2116; c) V. Bansal, A. Ahmad, M. Sastry, *J. Am. Chem. Soc.* **2006**, *128*, 14059 – 14066.

[9] a) Y. Jun, X. Y. Zhu, *J. Am. Chem. Soc.* **2004**, *126*, 13224 – 13225; b) S. D. Jacobsen, S. Demouchy, D. J. Frost, T. B. Ballaran, J. Kung, *J. Am. Mineral* **2005**, *90*, 61 – 70; c) X. Z. Du, W. G. Miao, Y. Q. Liang, *J. Phys. Chem. B* **2005**, *109*, 7428 – 7434; d) E. Biemmi, T. Bein, *Langmuir* **2008**, *24*, 11196 – 11202; e) Z. Liu, J. T. Robinson, X. M. Sun, H. J. Dai, *J. Am. Chem. Soc.* **2008**, *130*, 10876 – 10877; f) L. G. Kaake, Y. Zou, M. J. Panzer, C. D. Frisbie, X. Y. Zhu, *J. Am. Chem. Soc.* **2007**, *129*, 7824 – 7830.

[10] K. P. S. Dancil, D. P. Greiner, M. J. Sailor, *J. Am. Chem. Soc.* **1999**, *121*, 7925 – 7930.

[11] a) Y. He, H. T. Lu, L. M. Sai, Y. Y. Su, M. Hu, C. H. Fan, W. Huang, L. H. Wang, *Adv. Mater.* **2008**, *20*, 3416 – 3421; b) Y. He, H. T. Lu, Y. Y. Su, L. M. Sai, M. Hu, C. H. Fan, L. H. Wang, *Biomaterials* **2011**, *32*, 2133 – 2140.

[12] S. Godefroo, M. Hayne, M. Jivanescu, A. Stesmans, M. Zacharias, O. I. Lebedev, G. V. Tendeloo, V. V. Moshchalkov, *Nat. Nanotechnol.* **2008**, *3*, 174 – 178.

